Lunar Domes: Morphometric and Rheologic Properties

2

Abstract

This chapter describes different methods for determining the morphometric properties (diameter, height, flank slope, volume) of lunar domes, a model to estimate the physical properties of the dome-forming magma, and different classification schemes for lunar domes.

2.1 Observing Lunar Domes

The appearance of an "ideal" dome of hemispherical shape located on an even mare surface can be simulated based on image rendering, which provides an artificial image and thus yields the brightness distribution across the dome surface and the shape of the shadow (Fig. 2.1). The dome diameter is given by D and its height by h. Domes with a non-circular outline can be described by a major axis a and a minor axis b. We then define the dome diameter as the geometric mean $D = (ab)^{1/2}$ and its so-called circularity by $c = b/a$.

Based on this approach, it can be shown according to Lena et al. (2004) that lunar domes with their typically low flank slopes display a significant contrast with respect to the surrounding surface only when the solar elevation angle is lower than 4–5°. As shown in Fig. 2.1b, only slightly different solar elevation angles may result in strong differences in the simulated image of the dome and its shadow. For a dome located on a sloping surface, the shadow is longer than for a dome situated on an even surface when the surrounding surface is inclined away from the sun and is shorter otherwise (Fig. 2.2). If the dome is not hemispherical but has steep flanks and a flat surface, the shape and length of the shadow are different from those shown in Fig. 2.1.

The selenographic coordinates of a lunar dome and its diameter can be computed based on a telescopic CCD image e.g. using the freely available Lunar Terminator Visualization Tool (LTVT) software package by Mosher and Bondo (2012). This software relies on the Unified Lunar Control Network (ULCN) 1994 (Davies et al. 1994) or, in a more recent version, on the ULCN 2005 (Archinal et al. 2006). For each control point in this list, precise

R. Lena et al., *Lunar Domes*, Springer Praxis Books,
DOI 10.1007/978-88-470-2637-7_2, © Springer-Verlag Italia 2013

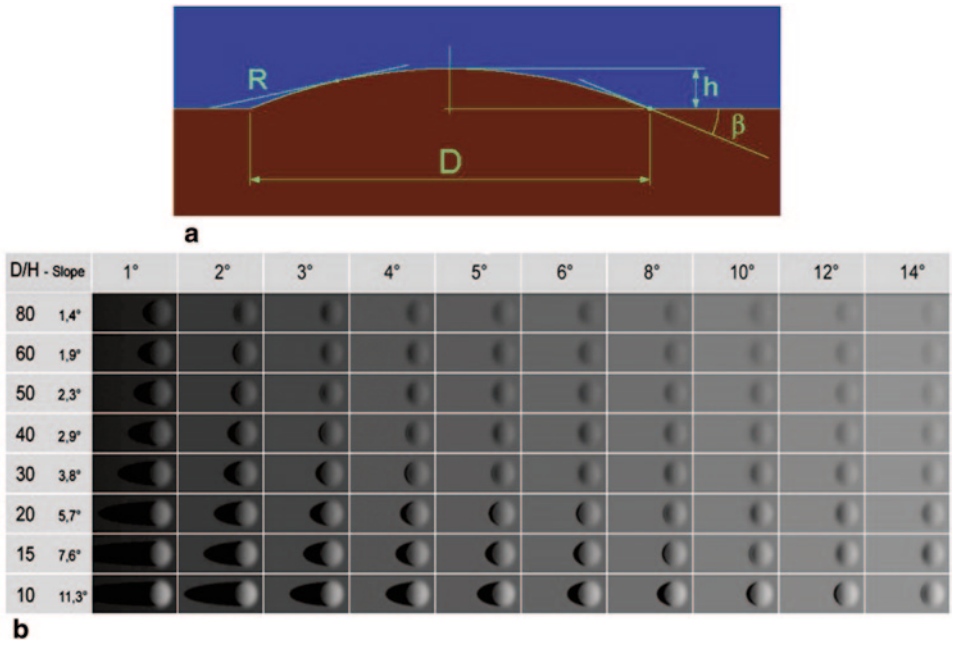

Fig. 2.1 **a** A lunar dome of diameter *D* and height *h*. **b** Model of an "ideal" dome with hemispherical cross-section located on a flat mare surface, rendered with the software developed by Lena et al. (2004). The appearance of a dome changes with increasing solar elevation

information about the selenographic coordinates and the elevation with respect to the average lunar radius is available. Marking some of these control points in a CCD image within the LTVT software then allows to read out selenographic coordinates for each image pixel.

2.2 Images Rendered Based on Topographic Data

Digital elevation models (DEMs) are of high importance for geologic interpretations. Most DEMs presented in this book were obtained based on an analysis of spacecraft or telescopic CCD images in terms of photoclinometry and shape from shading. These approaches rely on the fact that surface parts inclined towards the sun appear brighter than surface parts inclined away from it. The shape from shading approach aims for deriving the orientation of the surface at each image location by using a model of the reflectance properties of the surface and knowledge of the illumination conditions, finally leading to an elevation value for each image pixel (Horn 1990).

Inversely, a synthetic image of a dome can be generated based on an available DEM as seen from a given direction for lighting from some other specified direction. A global lunar DEM with a grid size of 1/1024 degree, obtained with the Lunar Orbiter Laser Altimeter (LOLA) instrument, has been released.[1] The LOLA instrument measures the distance

[1] http://pds-geosciences.wustl.edu/missions/lro/lola.htm.

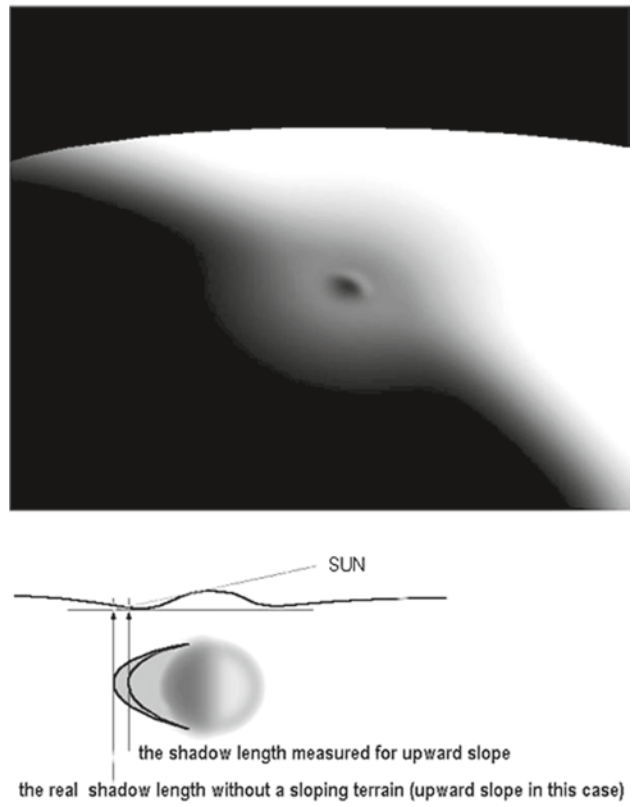

Fig. 2.2 The effect produced by a sloping soil on the shadow length: it will be either longer (*downward slope*) or shorter (*upward slope*) than on a flat surface

between the spacecraft and the lunar surface based on the time-of-flight of emitted laser pulses with a nominal accuracy of 0.1 m (Smith et al. 2010). The LTVT software can be used to generate synthetic views of selected parts of the LOLA DEM (Figs. 2.3 and 2.4).

The global LOLA DEM reveals many lunar domes and allows to estimate their diameters, approximate heights, and volumes. However, it is hardly possible to identify lunar domes in LOLA data alone, especially when they are situated on sloped terrain. In these cases, the dome shape and especially its diameter, which together with the height defines the flank slope, is not easily separable from the underlying terrain in the LOLA DEM. Additional images acquired at low solar elevation angles of no more than a few degrees are then required for an unambiguous identification of a dome based on its characteristic morphology.

2.3 Image-Based Photogrammetric Measurements

The Lunar Topographic Orthophotomaps, based on images acquired by the Apollo 15, 16, and 17 command modules with modified aerial cameras, were computed based on classical photogrammetric triangulation and represent lunar topographic data with elevation

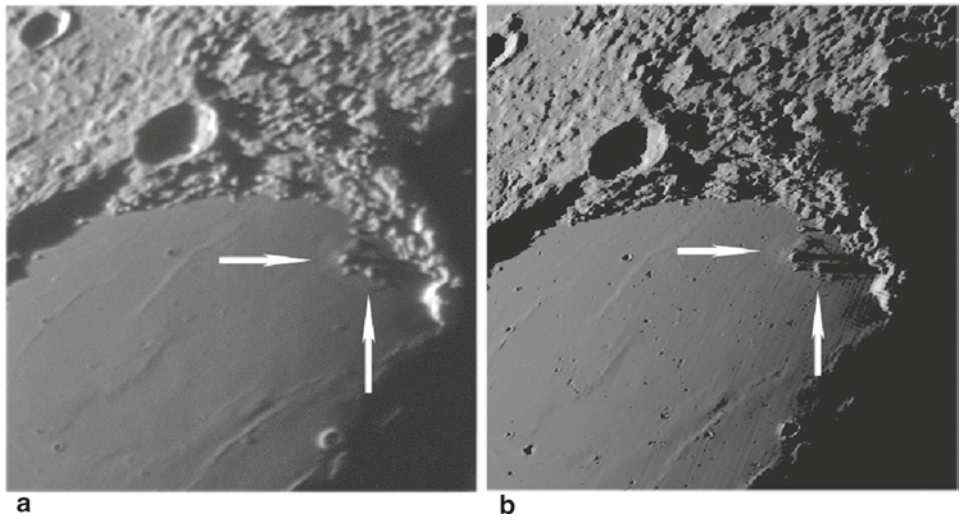

Fig. 2.3 **a** Telescopic image of a large domical feature in Sinus Iridum with several hills on top of it, image under late evening illumination. (Image by K. C. Pau). **b** Image rendered for the same illumination conditions based on the LOLA DEM

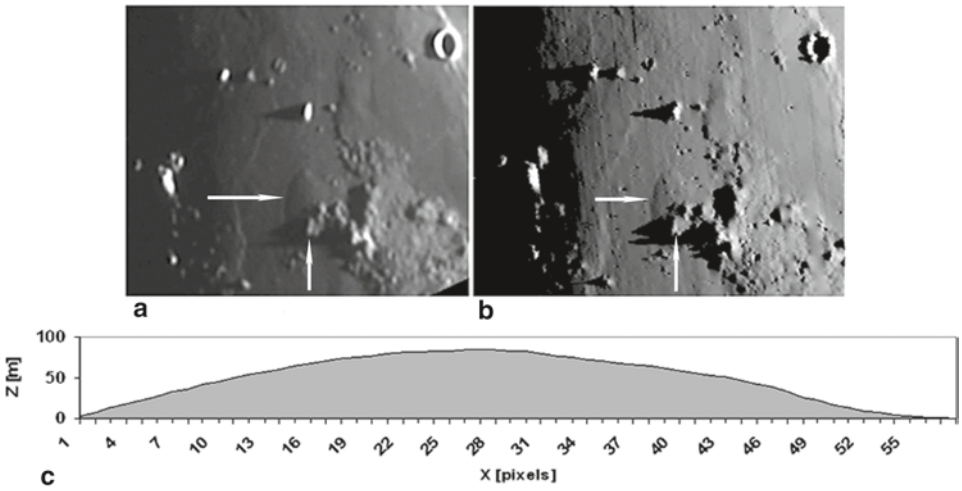

Fig. 2.4 **a** Telescopic image of a dome located near the crater Hansteen, termed Hansteen 2. (Image by J. Phillips taken under a solar elevation of 1.56°). **b** Image rendered for the same illumination conditions based on the LOLA DEM. **c** Cross-sectional profile of Hansteen 2 in east-west direction, obtained based on photoclinometry. The vertical axis is 20 times exaggerated. The effective dome height after subtraction of the spherical curvature amounts to 85 ± 10 m

standard errors of 30 m (Wu and Doyle 1990). They only cover a part of the lunar surface, mainly comprising Mare Serenitatis and Mare Tranquillitatis. Arya et al. (2011) present a DEM of one of the Marius Hills domes obtained using Chandrayaan-1 Terrain Mapping Camera (TMC) images. However, no statements are made about the lateral resolution and vertical accuracy of the DEM, and to our knowledge only one local TMC-based dome DEM has been published so far.

2.4 Determination of Morphometric Properties

2.4.1 Shadow Length Measurements

From the shadow length l corrected for foreshortening and a local solar elevation angle μ, the height h of a dome is given by

$$h = l \tan \mu. \tag{2.1}$$

The average flank slope angle ξ is then given by

$$\xi = \arctan\left(\frac{2h}{D}\right) \tag{2.2}$$

where D is the diameter of the dome and h its height.

The heights of more than 200 lunar domes were determined by Brungart (1964) based on telescopic lunar photographs by measuring shadow lengths, but his height estimates tend to be systematically too high. A possible reason is that on the high-contrast photographic reproductions of that time true shadows and shading effects could easily be confused. For example, for a dome (entry #30) on the floor of Capuanus crater (Capuanus 1, Fig. 1.7a), Brungart (1964) states a height of 376 m. Our shadow-based measurement yields a height of 100 ± 15 m for the same dome, consistent with the value obtained by the DEM construction approach described in Sect. 2.4.2.

A different shadow-based method for measuring lunar dome heights is introduced by Ashbrook (1961), who shows that the average slope of the dome flank equals the solar elevation angle when the shadow covers one quarter of the dome diameter, assuming a spherical surface of the dome. The observer determines the moment in time (corresponding to a known solar elevation angle ξ) for which this condition is met. The dome height is then readily obtained using Eq. 2.1 with $\mu = \xi$. The method by Ashbrook (1961) has primarily been devised for visual observations. The assumption of a spherical dome surface, however, represents a significant restriction. For the dome Milichius π (Fig. 2.5), a height of 742 m with an average slope of 9° is reported by Brungart (1964). We estimated the height of this dome with the method by Ashbrook (1961), yielding an average slope angle

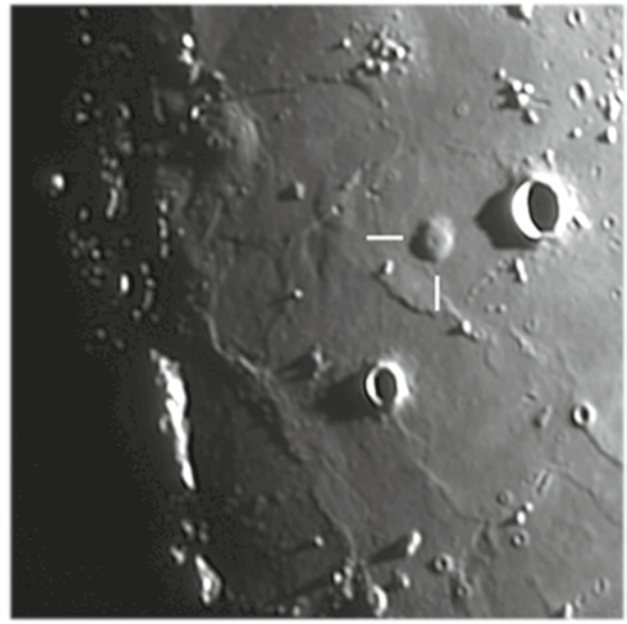

Fig. 2.5 Telescopic image of Milichius π (M12 in Fig. 1.5a) taken by J. Phillips (solar elevation 2.7°). The Ashbrook method yields a dome height of 220 ± 25 m

Table 2.1 Dome height and slope values determined using the shadow-based method by Ashbrook (1961) and the shape from shading approach (cf. Fig. 1.5 for identification of the domes)

	Ashbrook		Shape from shading	
Dome	Slope (°)	Height (m)	Slope (°)	Height (m)
C11	0.6	60	0.7	75
A2	1.5	310	1.5	330
H7	1.5	100	1.5	100
M11	2.8	150	2.8	150
M12	2.7	220	2.7	220

of 2.7° and a height of 220 m, which is found to be in good agreement with the photoclinometry and shape from shading analysis described in Sect. 2.4.2, resulting in a height of 220 ± 25 m. Slope and height values determined for some domes using the shadow-based method by Ashbrook (1961) and the shape from shading method are listed in Table 2.1.

As described in Sect. 1.6.5, some domes exhibit small embayed non-volcanic hills on their flanks (the dome V2 in Fig. 1.15b). Under sunrise and sunset illumination conditions, the hill on the dome V2 casts a shadow on the dome summit and on the surrounding surface, yielding height values of h_1 and h_2, respectively (Fig. 2.6). The height h of the dome is thus given by $h = h_2 - h_1$.

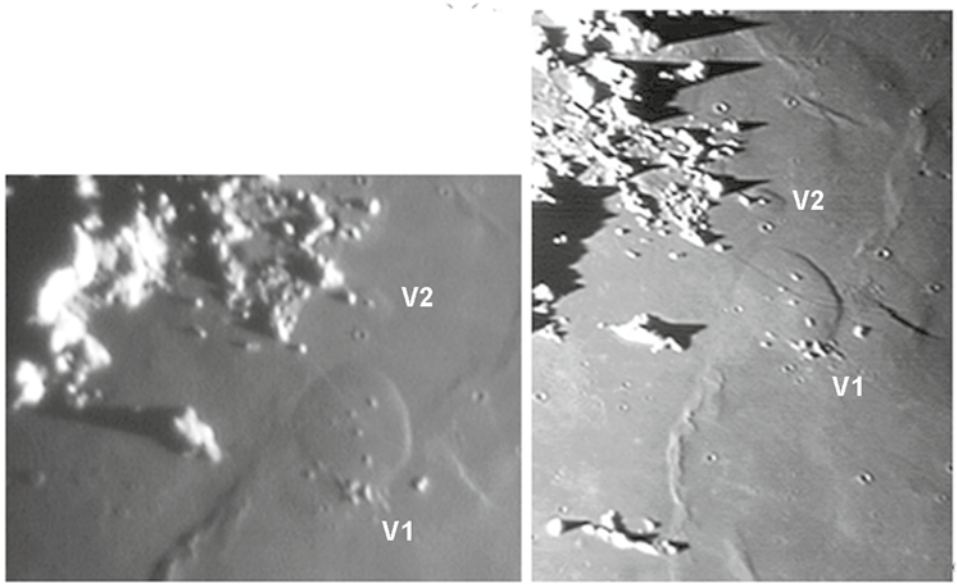

Fig. 2.6 Telescopic images of the Valentine dome and the dome V2, taken by K. C. Pau under opposite illumination (left image with solar elevation of 3.4° and right image with solar elevation of 3.2°, respectively). A height value of 76 m was derived by bidirectional evaluation of the length of the shadow cast by a hill on the surrounding mare surface under sunrise illumination ($h_2 = 336$ m) and on the dome summit under sunset illumination ($h_1 = 260$ m), respectively, implying a height of 76 m. The shape from shading method yields a dome height of 80 ± 10 m

2.4.2 Photoclinometry and Shape from Shading

Photoclinometric and shape from shading techniques have been proven to be suitable for the construction of local DEMs of the lunar surface, especially of low volcanic edifices. Since images acquired under solar illumination angles of less than a few degrees are required to reveal low domes, and because the current spacecraft image archives do not contain many images of this kind, we performed a reconstruction of the DEMs of a large set of lunar domes based on telescopic image data, relying on a combined photoclinometry and shape from shading approach.

The shape from shading method requires accurate knowledge of the reflectance properties of the surface material. The so-called Lambert model assumes perfectly diffuse scattering, implying an intensity R_L of scattered light according to

$$R_L(\rho, \theta_i) = \rho \cos \theta_i \tag{2.3}$$

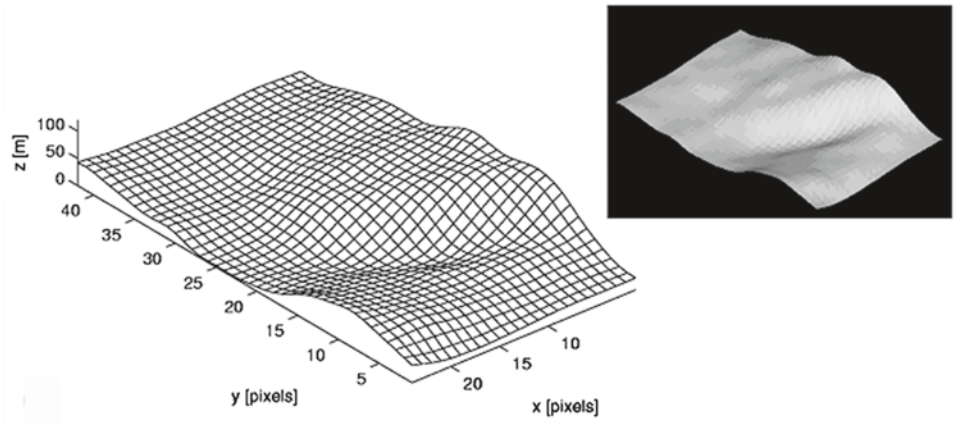

Fig. 2.7 DEM of the eastern flank of the dome V2 derived from Fig. 2.6 based on the shape from shading method (view from northeastern direction). The dome height corresponds to 80 ± 10 m. The curvature of the lunar surface has been subtracted

with ρ as the surface albedo and θ_i as the incidence angle between the normal vector of the surface and the illumination direction (Horn 1990). However, the Lambert model does not provide an accurate representation of the true scattering behaviour of the lunar surface. A much more appropriate relation is the physically motivated reflectance function by Hapke (1981, 1984, 1986, 2002) that is based on the theory of radiative transfer. It is not straightforward, however, to directly apply that model to 3D reconstruction (McEwen 1991). Therefore, in many remote sensing applications, the empirical lunar-Lambert law by McEwen (1991) is used according to

$$R_{LL}(\rho, \theta_i, \theta_e, \alpha) = \rho \left[2L(\alpha) \frac{\cos\theta_i}{\cos\theta_i + \cos\theta_e} + (1 - L(\alpha)) \cos\theta_i \right] \tag{2.4}$$

with θ_e as the emission angle between the normal vector of the surface and the viewing direction, and the lunar-Lambert parameter $L(\alpha)$ as an empirical value depending on the phase angle α between the illumination and the viewing direction. Given a suitable choice of $L(\alpha)$, the lunar-Lambert law fits the true scattering behaviour of a planetary surface similarly well as the Hapke model. Values of $L(\alpha)$ are given by McEwen (1991) for various kinds of planetary surfaces.

According to the method introduced by Horn (1990), the DEM is constructed by adjusting the gradients of the surface such that the average deviation of the observed and the modelled reflectance is minimised. The illumination direction and the viewing direction are known. An iterative optimisation scheme yields the surface gradient field along with

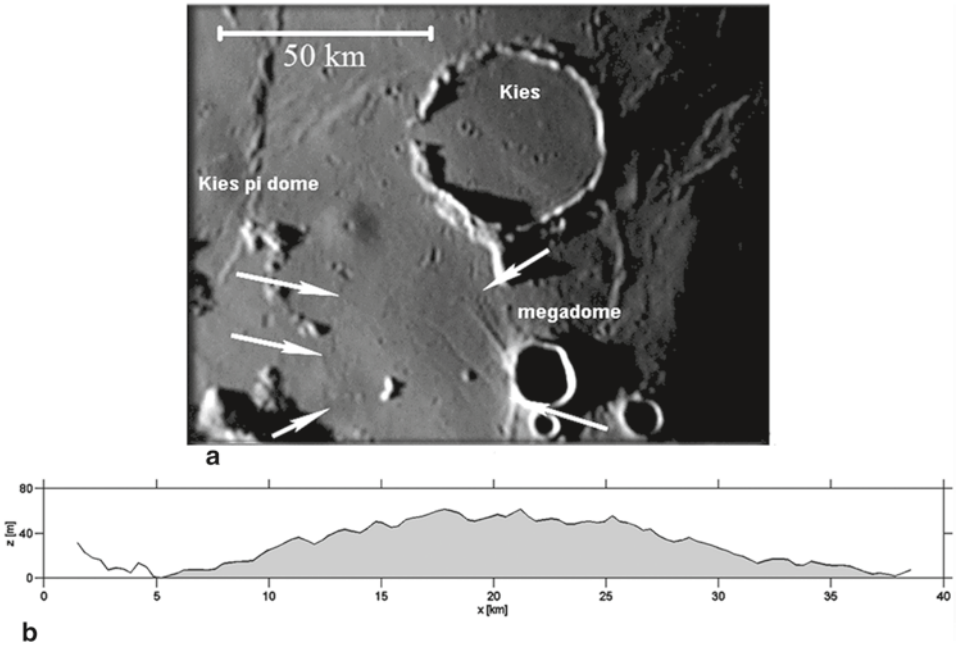

Fig. 2.8 **a** Telescopic image of the large dome Kies 2, located near the effusive dome Kies π. (Image by J. Phillips). **b** Cross-sectional profile of Kies 2 in east-west direction. The vertical axis is 50 times exaggerated, the curvature of the lunar surface has been subtracted. The height amounts to 55 ± 5 m. The rough shape of the surface is an artefact resulting from the image noise

the corresponding surface (i.e. the DEM) that fits best with the observed pixel intensities (Figs. 2.7 and 2.9).

The height h of a dome is obtained by measuring the elevation differences in the reconstructed DEM between the dome summit and the surrounding surface, taking into account the curvature of the lunar surface (Figs. 2.7–2.11). The dome volume V is computed by integrating the DEM over an area corresponding to a circular region of diameter D around the dome centre. If only a part of the dome surface can be reconstructed, e.g. due to the presence of shadows cast on the dome surfaces by nearby hills, the volume is estimated based on a cross-section in east-west direction through the centre of the dome, assuming rotational symmetry. A rough quantitative measure for the shape of the dome is given by the form factor $f = V/\left[h\pi(D/2)^2\right]$, where we have $f = 1/3$ for domes of conical shape, $f = 1/2$ for parabolic shape, $f = 1$ for cylindrical shape, and intermediate values for spherical shape.

The typical relative accuracy was found to correspond to 10 % for the dome height h and of 20 % for the volume V. A comprehensive catalogue of the morphometric properties of a large set of lunar domes is given by Lena and Wöhler (2011). Our dome height

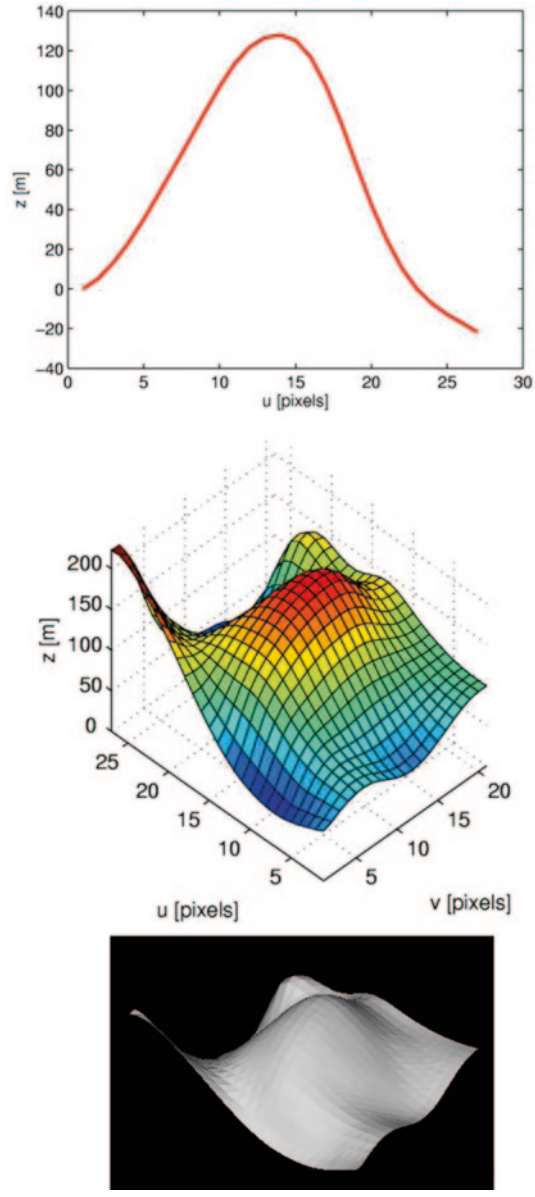

Fig. 2.9 DEM of the dome M11 obtained by means of the shape from shading method (Fig. 1.5a). Cross-section through the summit of the dome obtained with the photoclinometric approach (*top*), DEM viewed from the north-west (*middle*), and rendered view derived from the DEM (*bottom*, vertical axis 20 times exaggerated). The dome height amounts to 135 ± 20 m. The curvature of the lunar surface has been subtracted

values and those derived from the LOLA DEM commonly correspond to each other within less than a few percent. The modelling analyses about rheologic properties described in Sect. 2.5 mainly rely on dome heights inferred from low-sun images using the shape from shading technique. An advantage of the shape from shading approach is the fact that the image used for DEM construction can serve simultaneously for an accurate identification of the dome outline, while using the LOLA DEM would require the non-trivial registration of laser altimetry data and low-sun images.

http://www.springer.com/978-88-470-2636-0

Lunar Domes
Properties and Formation Processes
Lena, R.; Wöhler, C.; Phillips, J.; Chiocchetta, M.T.
2013, XIII, 174 p., Hardcover
ISBN: 978-88-470-2636-0